

Article

The Effect of Support on Catalytic Performance of Ni-Doped Mo Carbide Catalysts in 2-Methylfuran Production

Andrey Smirnov ^{1,2,*}, Ivan N. Shilov ¹, Maria V. Alekseeva ¹ , Olga A. Bulavchenko ¹, Andrey A. Saraev ¹ 
and Vadim A. Yakovlev ¹

¹ Federal Research Center Boreskov Institute of Catalysis, Lavrentyev Pr. 5, 630090 Novosibirsk, Russia; bykova@catalysis.ru (M.V.A.); isizy@catalysis.ru (O.A.B.); asaraev@catalysis.ru (A.A.S.); yakovlev@catalysis.ru (V.A.Y.)

² Technopark Kralupy, University of Chemistry and Technology Prague, Namesti G. Karse 7/2, 27801 Kralupy nad Vltavou, Czech Republic

* Correspondence: andrey.smirnov@vscht.cz; Tel.: +420-602-645-852

Abstract: Ni-doped Mo carbide with Ni/Mo atomic ratio of 0.1 was supported on SiO₂, Al₂O₃, and a porous carbon material (C), using a combination of gel combustion and impregnation methods. XRD, XPS, XANES, and EXAFS analyses indicated that the main active sites for the supported catalysts were metallic nickel and Mo carbides. The catalysts were evaluated in furfural hydrogenation to produce 2-methylfuran (2-MF) in a batch reactor at 150 °C under a hydrogen pressure of 6.0 MPa. The carbide materials supported on C showed the highest activity and selectivity towards 2-MF formation, with a yield of 61 mol.% after 3.5 h. Using furfuryl alcohol as the feedstock instead of furfural resulted in a high selectivity to 2-MF production. The carbon-supported sample was tested in a fixed-bed reactor at 160–260 °C with a pressure of 5.0 MPa in the hydrogenation of furfuryl alcohol, leading to the formation of up to 82 mol.% of 2-MF at 160–200 °C. The higher temperature (260 °C) resulted in the formation of C5 alcohols and hydrocarbons, while the hydrogenation of furfural at the same temperature led to 100 mol.% conversion, and up to an 86 mol.% yield of 2-MF.

Keywords: 2-methylfuran; furfural; furfuryl alcohol; fuel additive; molybdenum carbide; nickel molybdenum catalysts



Citation: Smirnov, A.; Shilov, I.N.; Alekseeva, M.V.; Bulavchenko, O.A.; Saraev, A.A.; Yakovlev, V.A. The Effect of Support on Catalytic Performance of Ni-Doped Mo Carbide Catalysts in 2-Methylfuran Production. *Catalysts* **2023**, *13*, 870. <https://doi.org/10.3390/catal13050870>

Academic Editor: Sara Fulignati

Received: 16 April 2023

Revised: 3 May 2023

Accepted: 8 May 2023

Published: 10 May 2023



Copyright: © 2023 by the authors. Licensee MDPI, Basel, Switzerland. This article is an open access article distributed under the terms and conditions of the Creative Commons Attribution (CC BY) license (<https://creativecommons.org/licenses/by/4.0/>).

1. Introduction

Currently, the processing of renewables contributes greatly to the sustainable development of civilization. In particular, the use of lignocellulosic biomass as a feedstock for producing fuels and their components has become an essential part of the development of the consumption of “eco” products [1].

Great attention has been given to 2-methylfuran (2-MF), since this compound could be produced by the hydrodeoxygenation of furfural [2]; it has promising properties for applications as a high-octane additive. A heating value of 2-MF equals 30.4 MJ/kg, and the blending research octane number (BRON) of 2-MF is 131 [3]. For comparison, the BRONs value for standard anti-knocking agents, such as ethanol or methyl tert-butyl ether, are equal to 128 and 135, respectively. In addition, 2-methylfuran has a low boiling point of about 64 °C, making it possible to use for easier engine starting in cold climates. 2-Methylfuran has the most attractive properties that characterize its compatibility with gasoline; moreover, it shows excellent solubility with fuels, in contrast with ethanol [4]. Therefore, 2-methylfuran is a promising fuel additive, and searching for a way to obtain this additive is a topical challenge for the industry.

2-Methylfuran is usually produced from furfural, which can be obtained from lignocellulosic feedstock through acidic hydrolysis [5,6]. The process is carried out by the sequential hydrogenation of furfural to furfuryl alcohol (FA), followed by the formation of 2-methylfuran. The reaction may be held in a gas or liquid phase, using homogenous and

heterogeneous catalysts [7]. The typical solid catalysts used for the production of 2-MF are Cu- or Cu-Cr-based systems, and catalysts based on noble metals [8].

High yields of 2-MF were reached using copper chromite supported on carbon material [9]. Nevertheless, Cu-Cr-based catalysts have several disadvantages, such as their rapid deactivation due to coke formation, changes in the oxidation state of the copper, and agglomeration of Cu particles under high temperature. Additionally, Cu-Cr-based systems have a detrimental effect on the environment, due to the high toxicity of Cr⁶⁺. Catalysts containing noble metals do not have these disadvantages. However, these catalytic systems usually lead to a low yield of 2-MF [10,11]. Moreover, the high cost of noble metals makes applying these catalytic systems less economically viable. Chromium-free transition metal systems can be used as alternative catalysts for the hydrogenation of furfural to 2-MF, which is possible because of the transition metals' low costs, high catalytic activity, and low toxicity [12,13]. However, these catalysts have low selectivity to 2-MF formation. Thus, the development of an efficient catalyst is still ongoing.

Recently, systems based on molybdenum carbides have shown high activity and selectivity toward target products in the hydroconversion of different molecules [14–16]. An essential feature of these catalysts is their ability to hydrogenate alcohol and carbonyl groups without reducing unsaturated carbon bonds and aromatic systems. This approach can be used to obtain 2-methylfuran. Lee et al. [17] studied molybdenum carbide in the hydrogenation of furfural in the gas phase. The authors indicated that the selectivity for 2-MF formation can reach 60% at temperatures of about 150 °C. Xiong et al. [18] also confirmed the high selectivity of molybdenum carbide for the production of 2-MF through high-resolution electron energy loss spectroscopy and density functional theory. In addition, the presence of a furan ring conjugated with an aldehyde group led to an additional loosening of the C=O bond, which also contributed to deoxygenation. A similar point of view was presented in the research of McManus et al. [19]. The authors noted that the Mo₂C/Mo(100) surface is active in the hydrodeoxygenation of adsorbed furfural to 2-MF, with preservation of the furan ring. Our previous research [15] with high-loading silica-stabilized molybdenum carbide catalyst indicated only 19% conversion of furfural during 3.5 h of reaction time over molybdenum carbide. Therefore, a modification of molybdenum carbide by a small amount of Ni was suggested to increase the activity to 100% conversion of furfural, with the formation of 30% of 2-MF. However, metallic Ni has high activity in the total hydrogenation of furfural with the formation of products from furan ring saturation. Thus, it was established that the atomic ratio of Ni/Mo in an Ni-doped Mo carbide catalyst must be lower than 1.0, in order to maintain high catalytic activity and maintain its high selectivity toward 2-MF formation.

Thus, nickel-doped molybdenum carbide catalysts are promising systems for the furfural hydrogenation of valuable chemicals, including 2-MF. Meanwhile, the production of 2-MF is typically carried out in a fixed-bed reactor, which indicates a necessity for catalyst molding. In contrast, considered Ni-doped Mo carbide systems have a total surface area in the range of 1–11 m²/g [14,15]. Therefore, the consideration of supported Ni-doped Mo carbide catalysts is an important topic for discussion. Hu et al. [20] used a molten salt method to synthesize self-supported nanoflower-like electrocatalysts composed of ultrathin Ni-doped Mo₂C nanosheets on carbon fiber paper. As a result, this catalytic system prepared at 1000 °C for 6 h exhibited an electrocatalytic performance for the hydrogen evolution reaction in 0.5 M H₂SO₄ that is comparable to that of commercial Pt/C and Ru-based systems [21,22].

In this study, we used a new approach, including a combination of gel combustion and wet impregnation methods for synthesizing supported Ni-doped Mo carbides. Furthermore, the effect of various supports (γ -Al₂O₃, SiO₂, and carbon) on the catalytic properties of Ni-doped Mo carbide catalysts in the production of 2-methylfuran was studied. The most promising carbide catalyst was used for the experiments in a fixed-bed reactor in the hydrogenation of furfural and furfuryl alcohol.

2. Results

2.1. Hydrogenation of Furfural on Supported $Ni_{0.1}MoC$ -Based Catalysts in a Batch Reactor

According to previous results [15], the atomic ratio of Ni/Mo in Ni–Mo carbide should be lower than 1.0, in order to retain high selectivity toward the formation of products with an unsaturated aromatic ring. In this case, the metal ratio Ni/Mo = 0.1 was chosen as the standard ratio for all Ni–Mo carbide catalysts in this study. Due to high-loading catalysts having a low surface area, they are poorly molded; thus, it is impossible to use such catalysts in industry. To solve this problem, $Ni_{0.1}MoC/X$ catalysts were prepared, where X is a solid support ($\gamma-Al_2O_3$, SiO_2 , and C). The amount of active phase $Ni_{0.1}MoC$ for all catalysts was 13 wt.%. The high-loading $Ni_{0.1}MoC-SiO_2$ catalyst was synthesized as a reference sample.

The catalysts were studied in the hydrogenation of furfural in a batch reactor at 150 °C and 6.0 MPa of hydrogen. According to the data obtained, the distribution of the reaction products from the reaction time is presented in Figure 1. The reaction was carried out for 210 min.

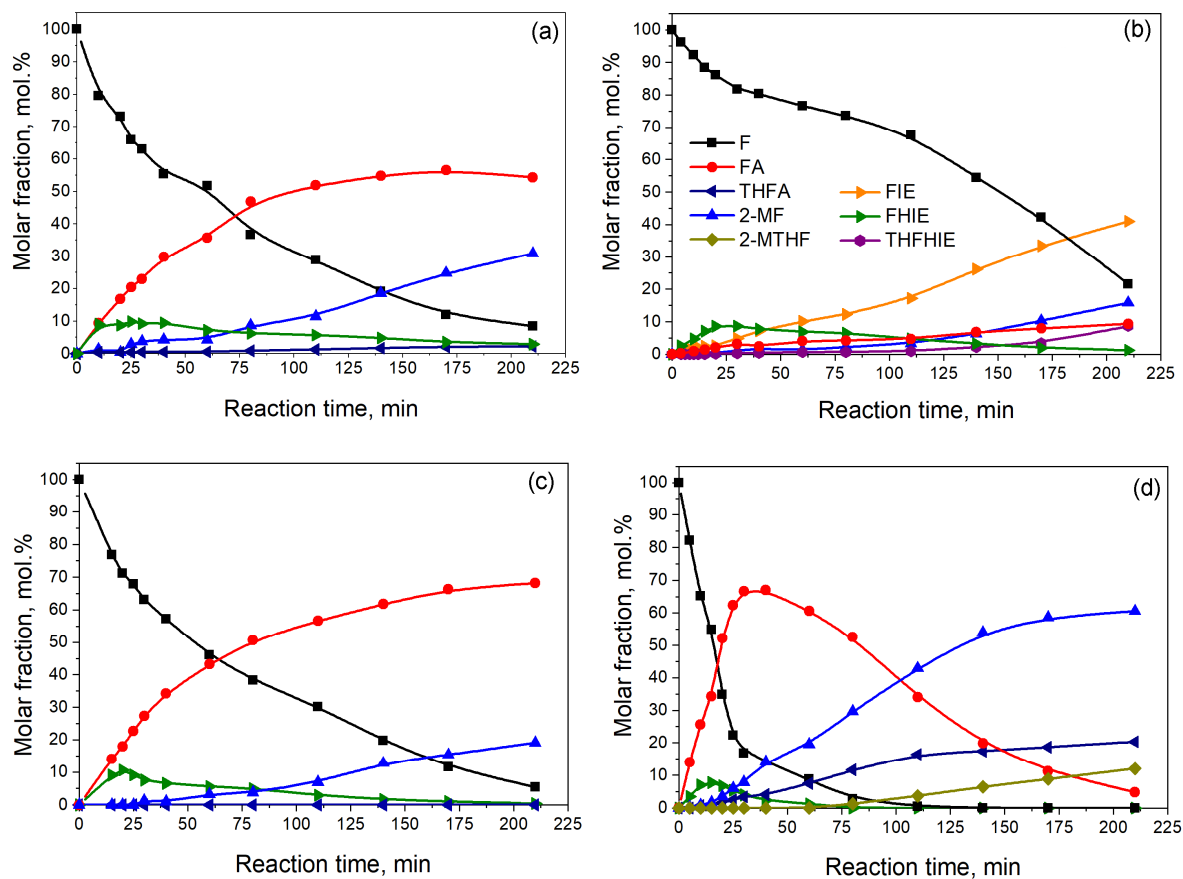


Figure 1. Dependence of the distribution of the reagent and product concentrations on the reaction time for furfural hydrogenation over (a) $Ni_{0.1}MoC-SiO_2$, (b) $Ni_{0.1}MoC/SiO_2$, (c) $Ni_{0.1}MoC/Al_2O_3$, and (d) $Ni_{0.1}MoC/C$ catalysts under the following reaction conditions: T = 150 °C, P = 6.0 MPa, $m_{cat} = 1.0$ g, and furfural concentration in solution with isopropanol equal to 3.5 vol.%. Abbreviations: F—furfural; FA—furfuryl alcohol; 2-MF—2-methylfuran; 2-MTHF—2-methyltetrahydrofuran; THFA—tetrahydrofurfuryl alcohol; FHIE—furfuryl-hydroxyl-isopropyl ether; FIE—furfuryl isopropyl ether; THFHIE—tetrahydrofurfuryl hydroxyl isopropyl ether.

According to the data obtained, the conversion of furfural on $Ni_{0.1}MoC-SiO_2$ at the end of the reaction was 92 mol.%, with the formation of 55 mol.% furfuryl alcohol (FA) and 31 mol.% 2-methylfuran (2-MF). Additionally, insignificant amounts (less than 1%) of tetrahydrofurfuryl alcohol (THFA) and 2-methyltetrahydrofuran (2-MTHF) were observed.

At the initial reaction stage, condensation of furfural and isopropyl alcohol led to the formation of furfuryl-hydroxyl-isopropyl ether (FHIE) up to 13 mol.%. Remarkably, after 25 min of the process, the concentration of FHIE decreased with furfural conversion. This fact indicates that the reaction of the formation of FHIE is reversible. The substance FHIE belongs to the class of hemiacetals. It is known that the formation of acetals and hemiacetals usually takes place under acidic catalysts [23]. In addition, it is known that molybdenum carbides have acidic properties [17], which contribute to FHIE formation.

It was shown that using supported samples led to catalytic performance that was similar to that for a high-loading sample. However, it must be considered that the active component loading for supported samples was 7 times less compared with $\text{Ni}_{0.1}\text{Mo-SiO}_2$. During furfural hydrogenation (up to 78 mol.% of conversion) over the catalyst $\text{Ni}_{0.1}\text{MoC/SiO}_2$, the yields of 2-MF and FA reached 15 mol.% and 9 mol.%, respectively. A major part of the reaction mixture (41 mol.%) was furfuryl isopropyl ether, which is formed during the etherification of furfuryl alcohol and isopropanol. It is well known that an etherification reaction usually takes place in the presence of acidic catalysts [24,25]. Furthermore, there are a couple of other products in small quantities, such as furfuryl-isopropyl ether (FIE) and tetrahydrofurfuryl-hydroxyl-isopropyl ether (THFHIE), which could be produced on acidic sites of the catalyst. As mentioned above, the molybdenum carbides have acidic sites. In addition, Liu et al. [26] showed that in $\text{MoO}_3/\text{SiO}_2$, a maximum of Lewis acid sites was reached at low MoO_3 loadings, while further deposition of MoO_3 decreased the total acidity. They concluded that amorphous MoO_3 provides more available Lewis acid sites on the catalyst surface than crystal MoO_3 . Rajagopal et al. [27] showed that deposition of MoO_3 on SiO_2 increased the acidity according to pyridine chemisorption at 473 K. This result is in agreement with [28].

Using $\text{Ni}_{0.1}\text{MoC/Al}_2\text{O}_3$ and $\text{Ni}_{0.1}\text{MoC/C}$ led to 95 mol.% and 100 mol.% conversion of furfural, respectively. Al- and C-based supports did not contribute to the formation of FIE compared to SiO_2 . After 210 min of reaction, the carbon-supported catalyst had 61 mol.% of 2-MF and 5 mol.% of FA, while the $\text{Ni}_{0.1}\text{MoC/Al}_2\text{O}_3$ catalyst promoted the formation of 19 mol.% of 2-MF and 68 mol.% of FA. The Ni-doped Mo carbide catalyst supported on carbon allowed up to 20 mol.% of THFA and 12 mol.% of 2-MTHF to be obtained. In general, the selectivity to 2-MF formation (28 mol.%) for carbon support was higher compared to that (12 mol.%) for Al_2O_3 at 95 mol.% for the conversion of furfural. It is remarkable that supported Ni-doped molybdenum carbide catalysts are compatible with noble metals supported on carbon. For example, Makela E. et al. [11] studied Pt and Ru catalysts supported on activated carbon in the liquid-phase hydrogenation of furfural. The maximum yield of 2-MF was found to be 48% at a temperature of 230 °C and a hydrogen pressure of 4.0 MPa. Fuente-Hernández et al. [29] obtained 41.6% of selectivity to 2-MF formation at 59.9% conversion of furfural at 300 °C and 1500 psi of hydrogen, using 3 wt.% of Pt supported on a maple-based biochar. They also mentioned that the nature of the solvent could change the hydrogenation rates and the formation of condensation products.

As mentioned above, the reaction scheme includes the sequential hydrogenation of furfural to furfuryl alcohol, followed by the formation of 2-MF. One way to increase the yield of 2-MF could be to change the initial reagent from furfural to furfuryl alcohol. Since $\text{Ni}_{0.1}\text{MoC/C}$ showed a high preference for 2-MF formation, it was chosen for the study in the hydroconversion of furfuryl alcohol under the same reaction condition. The distribution of reaction products is shown in Figure 2.

After 3.5 h of the reaction at 150 °C and hydrogen pressure of 6.0 MPa, the conversion of furfuryl alcohol reached 74 mol.%. The main product of the hydrogenation of furfuryl alcohol was 2-MF, with 58 mol.% of the yield. No saturated product, such as 2-methyltetrahydrofuran alcohol, was observed in the reaction mixture after 3.5 h. Moreover, the concentration of THFA was very low, and the maximum yield did not exceed 2 mol.%. The by-products of the hydrogenation of furfuryl alcohol were difurfuryl ether (DFE) and furfuryl-isopropyl ether. The latter was formed as a result of the polymerization of furfuryl alcohol on acidic sites of molybdenum carbide.

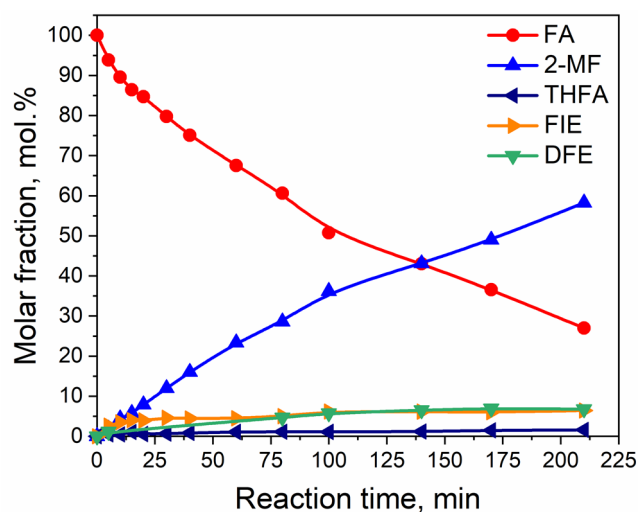


Figure 2. Dependence of the distribution of the reagent and products on the reaction time for hydrogenation of furfuryl alcohol over $\text{Ni}_{0.1}\text{MoC}/\text{C}$ under the following reaction conditions: $T = 150\text{ }^\circ\text{C}$, $P = 6.0\text{ MPa}$, $m_{\text{cat}} = 1.0\text{ g}$, and furfuryl alcohol concentration in the solution with isopropanol equal to 3.5 vol.%. Abbreviations: FA—furfuryl alcohol; 2-MF—2-methylfuran; THFA—tetrahydrofurfuryl alcohol; FHIE—furfuryl-hydroxyl-isopropyl ether; FIE—furfuryl isopropyl ether; DFE—difurfuryl ether.

In general, furfuryl alcohol could replace furfural in 2-MF production. However, the results showed that the conversion of FA is lower than the conversion of furfural under the same reaction conditions. The conversion of furfural probably includes two pathways for the formation of 2-MF. The first one is the sequential hydrogenation to FA followed by 2-MF formation, and the second one is direct hydrodeoxygenation of furfural to 2-MF.

Based on the observed results, catalyst $\text{Ni}_{0.1}\text{MoC}/\text{C}$ is considered to be promising for catalytic systems in furfural hydrogenation to 2-MF.

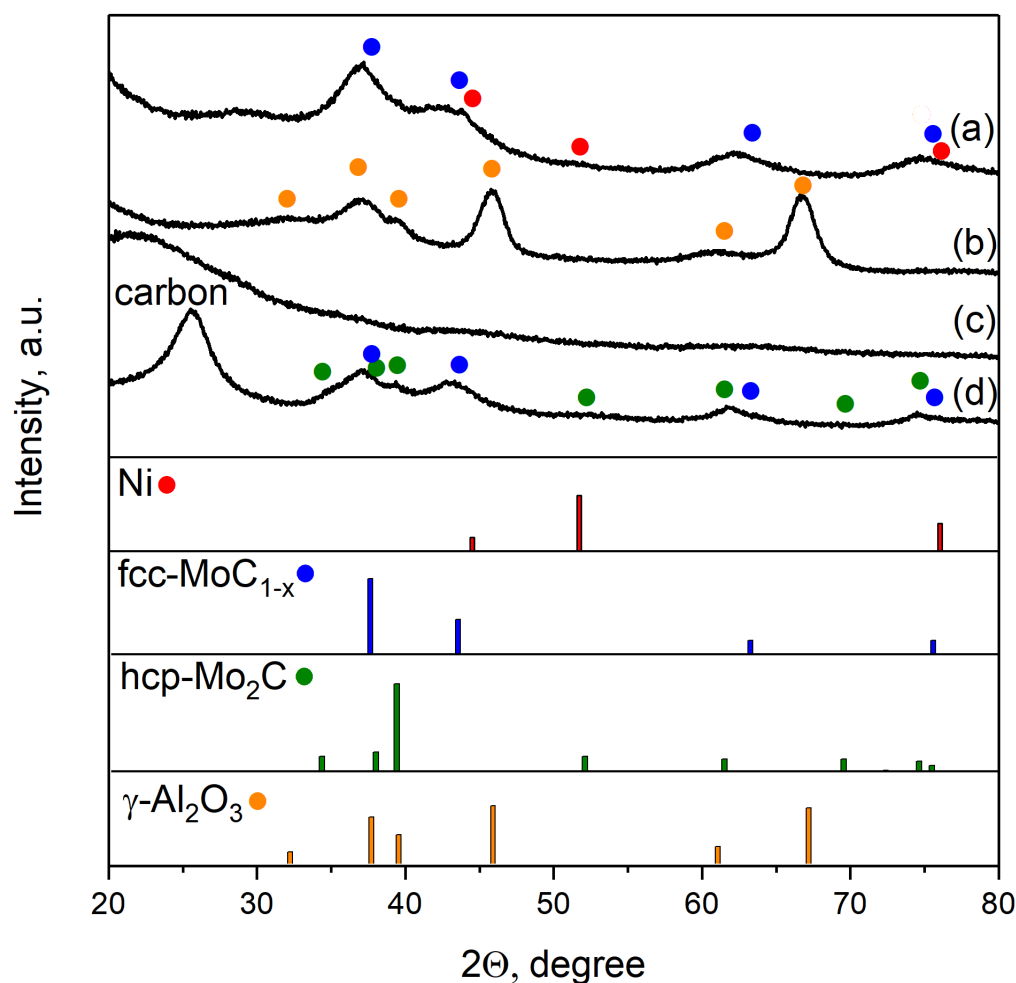
2.2. Characterization of $\text{Ni}_{0.1}\text{MoC}$ -Based Catalysts

The BET method was used to investigate the textural properties of the samples. The results are shown in Table 1. The $\text{Ni}_{0.1}\text{MoC}-\text{SiO}_2$ catalyst was represented by mesoporous material with a total surface area of around $11.3\text{ m}^2/\text{g}$, and an average pore diameter of 4.3 nm, which is in agreement with previous data [15]. The use of supports allowed us to increase the surface area by more than 10 times and increase the average pore diameter. Thus, the $\text{Ni}_{0.1}\text{MoC}/\text{SiO}_2$ sample had the highest surface area of $264\text{ m}^2/\text{g}$. The $\text{Ni}_{0.1}\text{MoC}/\text{Al}_2\text{O}_3$ catalyst had a surface area of $168\text{ m}^2/\text{g}$ and an average pore size of about 9.3 nm. At the same time, the $\text{Ni}_{0.1}\text{MoC}/\text{C}$ sample had a surface area of $148\text{ m}^2/\text{g}$ and an average pore size of 11.3 nm. The initial carbon material had a significantly larger surface area ($469\text{ m}^2/\text{g}$) and a smaller average pore diameter, about 6.4 nm. This difference in texture properties can be associated with both partial destruction of the carbon structure during catalyst reduction at $600\text{ }^\circ\text{C}$, and partial blocking of pores by NiMoC -based components.

Figure 3 contains the diffraction pattern of high-loading and supported catalysts. According to the XRD data for the $\text{Ni}_{0.1}\text{MoC}-\text{SiO}_2$ sample, wide reflexes from cubic molybdenum carbide fcc-MoC_{1-x} are observed at angles 2θ equal to 36.9° , 41.8° , 62.2° , and 74.5° . According to the Scherrer equation phase of fcc-MoC_{1-x} , the average crystallite size was 35 \AA , which is in agreement with the data obtained earlier for unpromoted molybdenum carbide [15]. The presence of two small peaks at angles 2θ equal to 44.5° and 52.0° , and could be interpreted as reflexes from dispersed nickel. Thus, the obtained sample $\text{Ni}_{0.1}\text{MoC}-\text{SiO}_2$ is likely to be an X-ray amorphous silicate matrix with frequent inclusions of molybdenum carbide crystallites and dispersed nickel particles.

Table 1. Textural properties of supports and Ni_{0.1}MoC-based catalysts.

Sample	Surface Area BET, m ² /g	Average Pore Diameter, nm
Ni _{0.1} MoC-SiO ₂	11.3	4.3
SiO ₂	365	7.4
γ-Al ₂ O ₃	205	10.2
C	469	6.4
Ni _{0.1} MoC/SiO ₂	264	7.1
Ni _{0.1} MoC/Al ₂ O ₃	168	9.3
Ni _{0.1} MoC/C	148	11.3

**Figure 3.** XRD patterns of Ni_{0.1}MoC-based catalysts: (a) Ni_{0.1}MoC-SiO₂; (b) Ni_{0.1}MoC/Al₂O₃; (c) Ni_{0.1}MoC/SiO₂; (d) Ni_{0.1}MoC/C. PDF no.: fcc-MoC_{1-x} [15–457]; hcp-Mo₂C [35–787]; Ni [4–850]; γ-Al₂O₃ [10–425].

Only broad peaks of supports were observed in XRD patterns for the Ni_{0.1}MoC/SiO₂ and Ni_{0.1}MoC/Al₂O₃ samples. The XRD profile of the Ni_{0.1}MoC/C catalyst had broad peaks corresponding to cubic molybdenum carbide fcc-MoC_{1-x}. In addition, there were increases in the background at angles 2θ equal to 39.3° and 42.6°. This could indicate the presence of small amounts of hexagonal molybdenum carbide hcp-Mo₂C in the catalyst. The data presented here demonstrate broad peaks of carbon. No nickel signals were observed. Most likely, Ni was in the metallic state or in the form of a NiMo alloy. Due to the sample Ni_{0.1}MoC/C being selected as the best catalyst for the production of 2-MF, it was additionally studied with transmission electron microscopy (TEM). The images from the electron microscope are presented in Figure 4.

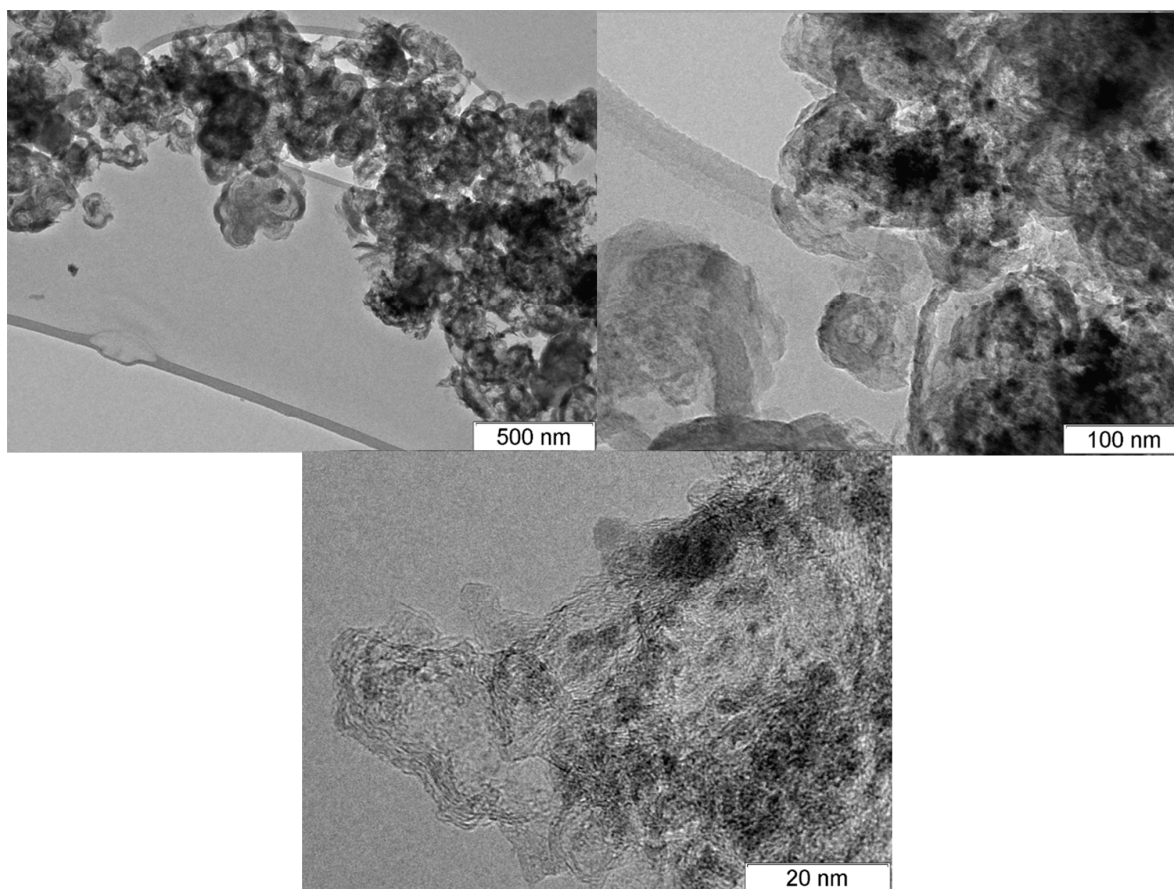


Figure 4. TEM images of the supported $\text{Ni}_{0.1}\text{MoC}/\text{C}$ sample.

According to the data obtained by TEM, the sample $\text{Ni}_{0.1}\text{MoC}/\text{C}$ was presented by particles of the active component that were observed in the form of contrasting round spots, with particles of sizes 2 to 30 nm deposited on the carbon matrix with a size range from 50 to 500 nm. The interplanar spacing of the supported particles (2.4 Å) corresponded to the crystal structure of hcp- Mo_2C (PDF number: 35-787). In addition, nanoparticles with sizes of about 0.3–1.0 nm were observed. According to energy-dispersive X-ray spectroscopy (EDX), these particles can be attributed to molybdenum oxides. At the same time, the composition of large particles corresponded to the stoichiometry of initial loading, where the atomic ratio of Ni/Mo is equal to 0.1.

Furthermore, the catalyst $\text{Ni}_{0.1}\text{MoC}/\text{C}$ was investigated using X-ray photoelectron spectroscopy (XPS). Lines corresponding to Mo, Ni, O, and C were detected in the XPS spectra. No other elements were found. The relative atomic concentrations of the detected elements are presented in Table 2.

Table 2. Relative atomic concentrations of elements on the surface of $\text{Ni}_{0.1}\text{MoC}/\text{C}$ catalyst.

Catalyst	[Ni]/[C]	[Mo]/[C]	[O]/[C]	[Ni]/[Mo]
$\text{Ni}_{0.1}\text{MoC}/\text{C}$	0.0017	0.019	0.11	0.088

The XPS data confirmed that the Ni/Mo ratio was close to 0.1, which corresponded to the initial loading of the metals. The presence of oxygen on the surface is explained by the formation of metal oxides during the passivation of the samples after reduction. Figure 5 shows the $\text{Ni}2p_{3/2}$ and $\text{Mo}3d$ spectra of the catalyst studied.

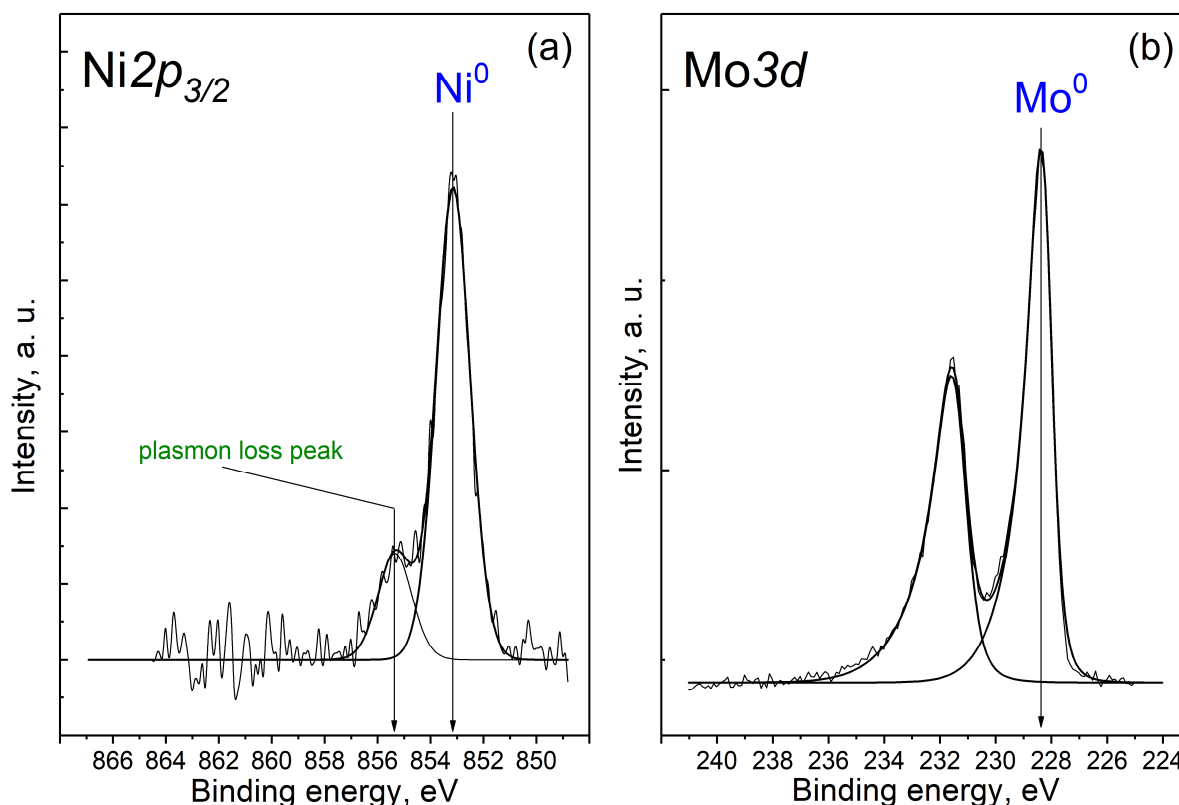


Figure 5. (a) Ni2p and (b) Mo3d core-level spectra of the Ni_{0.1}MoC/C catalyst.

The intense peak at 853.1 eV and a low-intensity peak of plasmon losses were observed in the spectrum for Ni2p_{3/2}. The binding energy (853.1 eV) and the shape of the spectrum correspond to nickel in the metallic state [30,31]. In the spectrum of Mo3d, there is only one doublet Mo3d_{5/2}-Mo3d_{3/2} with a binding energy in the region of 228.4 eV, which corresponds to Mo⁰ [32]. Nevertheless, it was hardly possible to distinguish molybdenum in the form of a metal or carbide on the basis of the XPS data. It is most likely that Mo presented as a carbide, in accordance with the XRD and TEM results.

Since XRD analysis is unable to detect molybdenum carbide or nickel spaces in the case of samples supported with alumina and silica, the XANES and EXAFS methods were used to characterize the Ni_{0.1}MoC/Al₂O₃ and Ni_{0.1}MoC/SiO₂ catalysts. Figure 6 presents XANES spectra for the samples obtained based on reference samples and Ni and Mo.

The absorption edge was determined from the maximum of the first derivative of the XANES spectra; for metallic molybdenum, the absorption edge was at 20,000 eV [33]. The XANES spectra of the Mo K-edge of the studied samples (Ni_{0.1}MoC/Al₂O₃, Ni_{0.1}MoC/SiO₂, and Mo₂C/SiO₂) had a similar shape, which is close to the spectrum of Mo₂C-SiO₂. This suggests that the samples contain molybdenum carbide. However, by this method, it is not possible to establish which type of carbide (fcc-MoC_{1-x} or hcp-Mo₂C) the catalysts contained. The Mo K-edge in the spectra of the samples under study was shifted, relative to the absorption edge of metallic molybdenum, by 6 eV towards higher energies; this was due to the transfer of a negative charge from molybdenum in Mo₂C to the support [34,35]. The Ni_{0.1}Mo/Al₂O₃ spectrum sample showed a small shoulder at the absorption edge in the region of 20,007 eV. Such a feature in the XANES spectra is observed when electronic transitions occur from 1s to 4d and 5p hybridized molecular orbitals of molybdenum mixed with 2p orbitals of oxygen. The mixing occurs due to the centrosymmetric environment of molybdenum atoms with oxygen atoms [36]. A similar shoulder at the absorption edge was observed in the spectrum of MoO₃, while in the spectrum of MoO₂, such a shoulder was not observed. Molybdenum oxide MoO₃ has a layered structure consisting of distorted molybdenum octahedra [MoO₆] combined into double layers, where molybdenum is in

the oxidation state 6+ [37]. Molybdenum oxide, MoO_2 , where molybdenum is in the 4+ oxidation state, has a disordered rutile-type structure. From the analysis of the XANES spectrum of the K absorption edge of molybdenum, it can be argued that the samples contain molybdenum in the oxidation state 6+. No clear edges were found for MoO_2 .

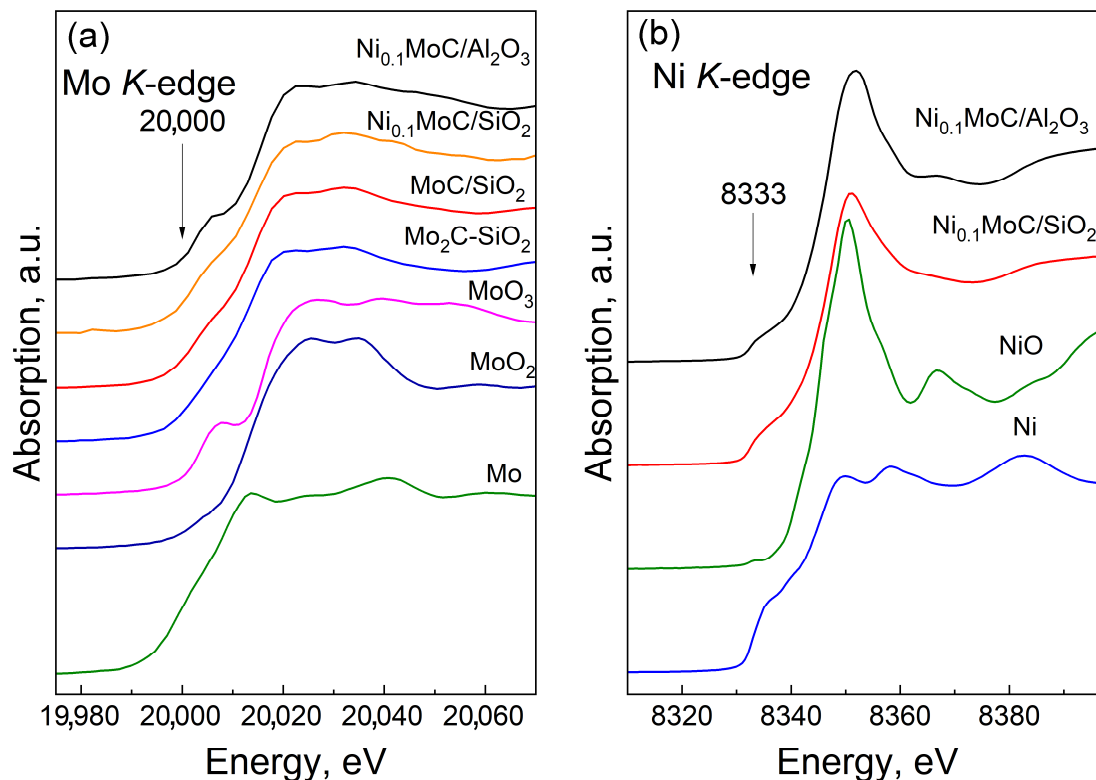


Figure 6. XANES spectra at (a) Mo K-edge and (b) Ni K-edge of the $\text{Ni}_{0.1}\text{MoC}/\text{Al}_2\text{O}_3$ and $\text{Ni}_{0.1}\text{MoC}/\text{SiO}_2$ samples. The spectra of the reference samples (Mo, MoO_2 , MoO_3 , $\text{Mo}_2\text{C-SiO}_2$, Ni, and NiO) are provided for comparison.

The K-edge of metallic nickel corresponded to 8333 eV [33]. The XANES spectrum of metallic nickel is characterized by the presence of two peaks in the region of 8350–8360 eV of approximately the same intensity at the K-edge, as well as a pre-edge feature in the form of a shoulder in the region of 8335 eV ($1s \rightarrow 3d$ transition). In contrast to the XANES spectrum of metallic nickel, the NiO spectrum had an intense peak at the absorption edge in the region of 8350 eV [36,38]. The XANES spectra of the Ni K-edge of the catalysts had a pronounced peak at 8351.0 eV, which is characteristic of NiO, the XANES spectra of nickel oxide. The spectra of the samples under study also exhibited a near-edge characteristic in the form of a shoulder at 8335 eV, which is characteristic of the XANES spectrum of nickel foil. We can assume the existence of a mixture of two phases of nickel in the metallic and oxidized states in the samples. However, the possibility of the presence of nickel carbide particles in the samples studied should not be ruled out, as the XANES spectrum of nickel carbide was similar to that of metallic nickel [39]. Two peaks in the region of 8350–8360 eV of approximately the same intensity in the metallic nickel changed their intensity when carbon was added. The peak at 8350 eV decreased, and the peak at 8360 eV increased; thus, an intense peak remained in the Ni_3C nickel carbide Ni_3C , with a maximum in the region of 8360 eV.

Table 3 shows the results of the XANES modelling of the spectra of the samples into a linear combination of the spectra of reference samples (Mo, MoO_2 , MoO_3 , $\text{Mo}_2\text{C-SiO}_2$, and Ni, NiO). As a result of the decomposition of the K-absorption edge spectra from Mo of the studied samples into a linear combination of the spectra of the reference sample spectra, it was found that in the $\text{Mo}_2\text{C}/\text{SiO}_2$ sample, approximately 75% of molybdenum was in the

composition of molybdenum carbide; the rest of the molybdenum was in the Mo^{6+} state in the composition of the MoO_3 . The $\text{Ni}_{0.1}\text{MoC}/\text{SiO}_2$ sample decomposed into a linear combination of Mo, MoO_3 , and $\text{Mo}_2\text{C}-\text{SiO}_2$ in a ratio of 10:34:56. In the $\text{Ni}_{0.1}\text{MoC}/\text{Al}_2\text{O}_3$ sample, molybdenum was in the composition of MoO_3 and Mo_2C in a ratio of approximately 58:42. No metallic component of molybdenum was found in $\text{Ni}_{0.1}\text{MoC}/\text{Al}_2\text{O}_3$.

Table 3. Relative atomic concentrations of elements on the catalyst surface.

Sample	Mo K-Edge				Ni K-Edge	
	Mo, %	MoO_2 , %	MoO_3 , %	Mo_2C , %	Ni, %	NiO, %
$\text{Ni}_{0.1}\text{Mo}/\text{Al}_2\text{O}_3$	0	0	58	42	32	68
$\text{Ni}_{0.1}\text{Mo}/\text{SiO}_2$	10	0	34	56	49	51
$\text{Mo}_2\text{C}/\text{SiO}_2$	0	0	25	75	-	-

An analysis of the Ni K-edge showed that, in the $\text{Ni}_{0.1}\text{Mo}/\text{Al}_2\text{O}_3$ sample, approximately 68% of nickel atoms were in the NiO composition, and approximately 32% were in the metallic state (the possible presence of nickel carbide was not taken into account). In the $\text{Ni}_{0.1}\text{Mo}/\text{SiO}_2$ sample, the nickel atoms had a local environment similar to NiO and Ni in approximately equal proportions (51% and 49%). The presence of nickel carbide could not be established due to the absence of the XANES spectrum of bulk Ni_3C .

Therefore, the $\text{Ni}_{0.1}\text{Mo}/\text{Al}_2\text{O}_3$ sample contained a large amount of molybdenum and nickel oxides, molybdenum carbide, and nickel in the metallic state. The $\text{Ni}_{0.1}\text{Mo}/\text{SiO}_2$ sample also contained molybdenum and nickel oxides, but their proportions in this sample were lower than that of $\text{Ni}_{0.1}\text{Mo}/\text{Al}_2\text{O}_3$, indicating its better oxidation resistance. In addition to oxides, this sample contains molybdenum carbide, nickel, and molybdenum in the metallic state; therefore, the possibility of forming a nickel-based bimetallic Ni-Mo compound could not be ruled out. However, in order to determine the presence and composition of bimetallic particles, a larger amount of this component is necessary.

The EXAFS Fourier transforms of the K-edge Mo (a) and Ni (b) of the studied samples are shown in Figure 7. For the $\text{Ni}_{0.1}\text{Mo}/\text{Al}_2\text{O}_3$, $\text{Ni}_{0.1}\text{Mo}/\text{SiO}_2$, and $\text{Mo}_2\text{C}/\text{SiO}_2$ samples, peaks in the regions of 1.1 Å and 1.6 Å were observed that corresponded to the Mo–O distances for MoO_3 . This indicates that there was no local ordering beyond 3 Å in the samples under study, i.e., molybdenum oxide was probably in an amorphous state, either in the form of a thin film or in a highly dispersed state. Obtained data confirmed the presence of amorphous MoO_3 on the SiO_2 , providing more available Lewis acid sites on the catalyst, and promoting the esterification reaction. A peak at 2.5 Å (for metallic molybdenum) was observed in the EXAFS curves of the $\text{Ni}_{0.1}\text{Mo}/\text{SiO}_2$ and $\text{Mo}_2\text{C}/\text{SiO}_2$ samples, as well as $\text{Mo}_2\text{C}-\text{SiO}_2$. Taking into account the results of the analysis of the XANES spectra, it can be argued that, on the EXAFS curves of the studied $\text{Ni}_{0.1}\text{Mo}/\text{SiO}_2$ and $\text{Mo}_2\text{C}/\text{SiO}_2$ samples, the main contribution to the peak at 2.5 Å comes from the Mo–Mo scattering paths in the Mo_2C structure. In the curve of the $\text{Ni}_{0.1}\text{Mo}/\text{Al}_2\text{O}_3$ sample, the peak at 2.5 Å, related to the Mo–Mo distance, is of low intensity; therefore, the molybdenum carbide was present in a highly disordered form.

At the edge of nickel absorption in the $\text{Ni}_{0.1}\text{MoC}/\text{Al}_2\text{O}_3$ and $\text{Ni}_{0.1}\text{MoC}/\text{SiO}_2$ samples, two peaks were observed in the regions of 1.6 and 2.2 Å, which corresponded to the Ni–O distance in nickel oxide and the Ni–Ni distance in metallic nickel. This confirmed the presence of nickel in the sample in two forms. However, in nickel oxide, there was an intense peak at 2.6 Å that corresponded to the Ni–Ni distance, which was not observed in the EXAFS curves. From this, we can conclude that the local order in the oxide component of nickel-containing samples was formed only within ~2 Å. With a high probability in the samples, nickel oxide, like molybdenum oxide, is in an amorphous state, either in the form of a thin film or in a highly dispersed state.

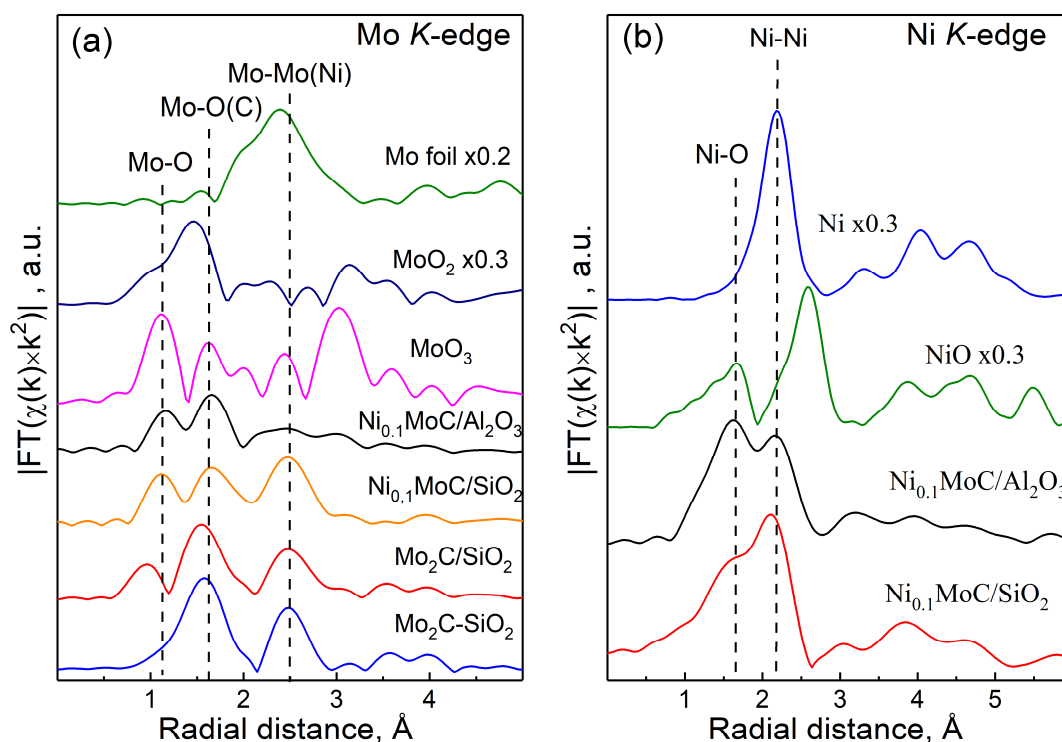


Figure 7. EXAFS Fourier transforms of the (a) Mo and (b) Ni K-edges of the studied samples in comparison with the spectra of the reference samples Mo, MoO₂, MoO₃, Mo₂C-SiO₂, Ni, and NiO.

Based on the analysis of the XANES spectra, it can be concluded that the Ni_{0.1}MoC/Al₂O₃ and Ni_{0.1}MoC/SiO₂ samples contain metallic Ni. Most of the active metals were found in oxidic or carbide forms. The metal oxides and carbides included in the composition of the samples were in a highly amorphous state. Oxides could be formed due to the interaction of metals with atmospheric oxygen after the reduction stage.

Thus, it was found that the composition of the active component of supported carbide catalysts includes molybdenum carbides, Ni and Mo oxides, and metallic nickel. This is in agreement with the XRD and TEM data obtained for the sample with carbon as support.

2.3. Hydrogenation of Furfuryl Alcohol and Furfural on Ni_{0.1}MoC/C Catalyst in a Flow Reactor

Considering that Ni_{0.1}MoC/C showed the best catalytic performance for 2-MF production, this catalyst was studied in the hydrogenation of both furfural and furfuryl alcohol in a fixed-bed reactor. The last one was chosen as a feedstock for screening of different reaction temperatures, due to the formation of a minimal amount of side products during 2-MF production in the batch reactor. To investigate the stability of the catalyst, the experiments were performed without solvent, and the furan derivatives were not subjected to additional purification before the experiments. The samples were taken every hour. However, no products were observed in the collector system after 1 h.

In the first stage, the process was carried out at different temperatures (160, 200, and 260 °C) at 5 MPa of hydrogen and LHSV = 1 h⁻¹ for 7 h of time on stream (TOS) using furfuryl alcohol (molar ratio H₂/FA = 23). The data obtained on the effect of reaction temperature on the selectivity and activity of Ni_{0.1}MoC/C are presented in Figure 8.

At temperatures of 160 °C, the initial conversion was 83 mol.% and increased to 99 mol.% at 4 h of the reaction, followed by a decrease in the conversion to 96 mol.% at 7 h of TOS. This dependence could be related to the additional activation of the metallic active component during the beginning of the reaction under high-pressure hydrogen, with subsequent deactivation of the catalyst due to the formation of polyfurans. For example, the yield of the condensation products of two furanic molecules reached up to 9.6 mol.%

in the reaction mixture after 7 h of TOS. The main product was 2-MF with the selectivity of the formation of 82 mol.% after 7 h of TOS. During the reaction, a decrease in the selectivity of 2-MTHF from 28 mol.% to zero was observed, which also confirmed the catalyst's deactivation. The selectivity of the THFA formation was kept the same during TOS (6 mol.%).

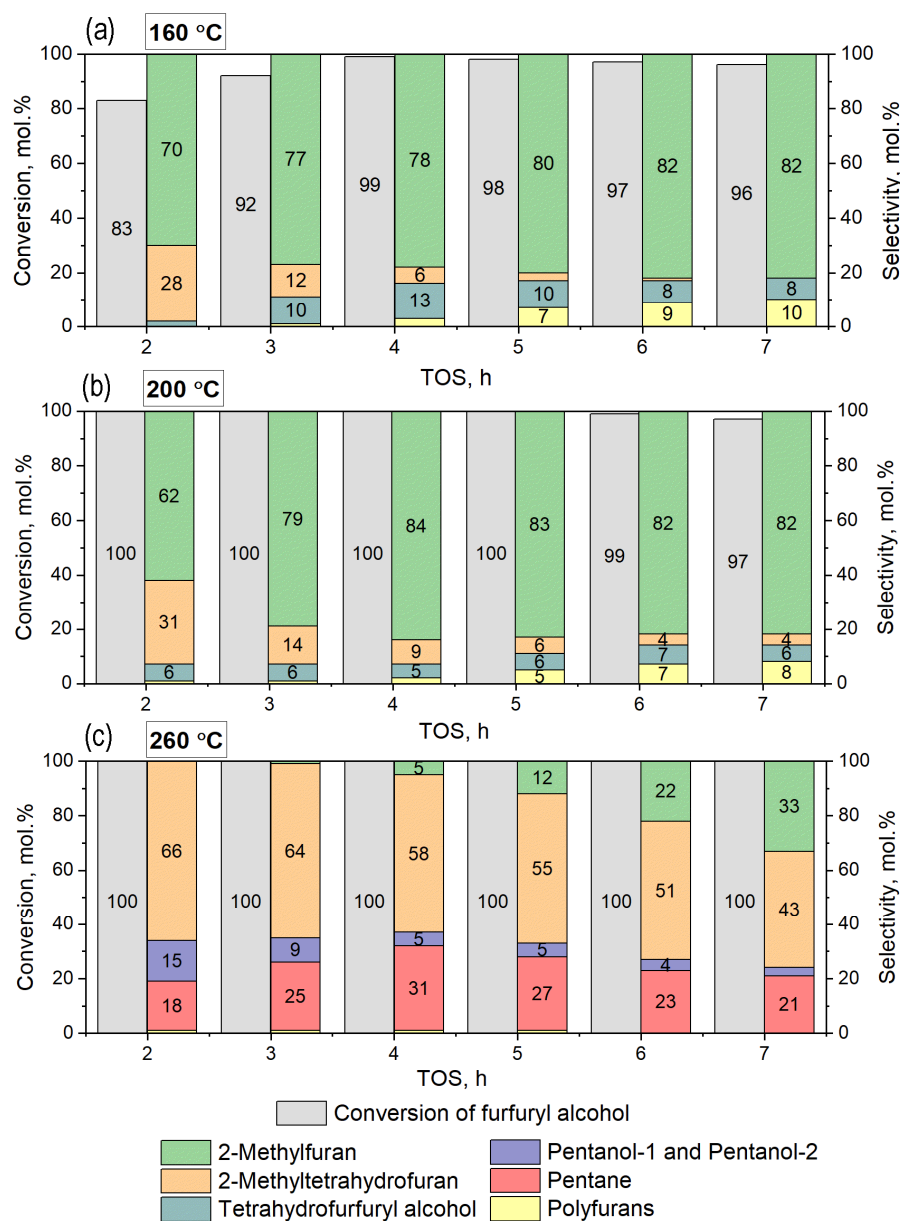


Figure 8. Conversion and selectivity toward the formation of products during the hydrogenation of furfuryl alcohol on the Ni_{0.1}MoC/C catalyst. Reaction conditions: temperatures (a) 160 °C, (b) 200 °C, (c) 260 °C; P = 5.0 MPa, m_{cat} = 1.9 g, LHSV = 1 h⁻¹, H₂/feedstock molar ratio = 23.

The use of a higher reaction temperature of 200 °C did not dramatically change the catalytic performance of the catalyst, leading to a slight increase in FA conversion with the same reaction products and selectivity similar to the production of 2-MF, 2-MTHF, THFA, and difurans. In general, the results obtained in the flow reactor at 160–200 °C were in agreement with the results in the batch reactor. The main difference was the presence of bifurans, the formation of which was suppressed in the batch reactor because of a high amount of solvent that prevented the condensation of furanic molecules.

Finally, several side reactions occurred at a high temperature of 260 °C. At this temperature, the total conversion of FA was established with the formation of 2-MTHF as the main product. The yield was 66 mol.% at the beginning, and 43 mol.% after 7 h of TOS. Along with hydrogenation and hydrodeoxygenation, the opening of the furanic ring with the appearance of pentanol-1, pentanol-2, and pentane was one of the main reactions. The maximum yield of pentane was 31 mol.%. This change in the product distribution and availability of new reaction pathways may have been caused by the use of high temperature, transferring the reaction into a gas phase reaction. The boiling point of furfuryl alcohol is 170 °C under standard pressure.

A decrease in FA conversion was observed during all temperatures considered. CHNS analysis of the Ni_{0.1}MoC/C sample before and after the test showed that the carbon deposit formation during FA hydrogenation occurred nonhomogeneously over the catalyst volume. A likely explanation could be the uneven distribution of the pore sizes in the carbon structure. For temperatures of 160 and 200 °C, the amount of carbon deposits in the catalyst were 2.4 and 3.1 wt.%, respectively. At a temperature of 260 °C, the carbon amount formed during the reaction reached 6.7 wt.%.

In the next stage of the research, the Ni_{0.1}MoC/C catalyst was studied directly in the furfural hydrogenation process. Taking into account the tendency of furfural to condense under high temperatures, the process was carried out without using a solvent, at a temperature of 260 °C, for 30 h to study the stability of the catalyst. The results are presented in Figure 9.

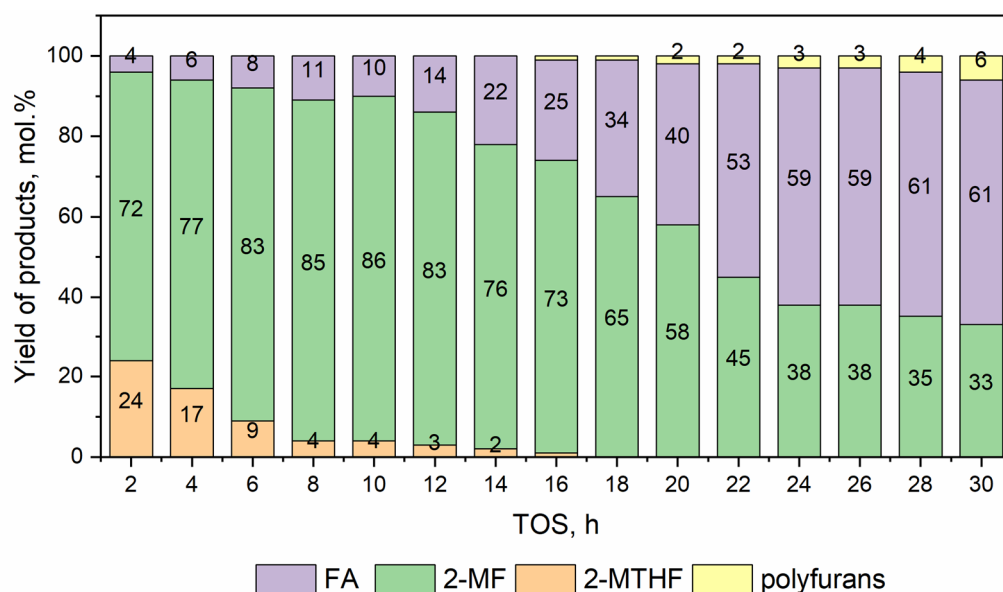


Figure 9. Yields of products formed during hydrogenation of furfural on Ni_{0.1}MoC/C catalyst. Reaction conditions: T = 260 °C, P = 5.0 MPa, m_{cat} = 1.9 g, LHSV = 1 h⁻¹, H₂/feedstock molar ratio = 23.

Throughout the process, the conversion of furfural was kept at 100 mol.%. The main products of furfural conversion under the chosen reaction conditions were 2-MTHF, 2-MF, and FA. In addition, after 14 h, the appearance of furfural (difurans) self-condensation products was observed, the yield of which in the reaction mixture increased to 6 mol.% by the end of the reaction. Despite the complete conversion of the feedstock throughout 30 h, a gradual drop in catalyst activity was observed according to the product distribution. The decrease in the yield of 2-MTHF as a product of the complete hydrogenation of furfural was observed. The yield of the target product 2-MF also decreased, from the maximum achieved value of 87 mol.% up to 35 mol.% after 30 h of TOS. The use of carbide catalysts has an advantage over transition metal catalysts. For example, Guerrero-Torres et al. [40] tested Cu-based catalysts supported on sepiolite in vapor-phase hydrogenation of furfural,

which reached a maximum furfural conversion above 80% after 5 h of reaction at 230 °C and 48% of the yield of 2-MF using 1CuZnO-Sepiolite catalyst.

The study of the spent catalyst via CHNS analysis revealed 14.3 wt.% of carbon deposits, presumably representing a mixture of condensation products of furfural and FA, which is one of the main reasons for the catalyst deactivation.

In general, Ni-doped molybdenum carbide supported on carbon showed high activity in furfural conversion, and a high yield of 2-MF. However, deactivation of the catalyst was observed. Further research may be aimed at improving the stability of the catalyst. Several approaches may be used, one of which involves modification of the support to control the activity of the catalyst and its stability. German et al. [41] showed that the catalytic performance of the catalysts based on carbon support (Sibunit) with diazonium salts of Pd and Pd-Au in furfural hydrogenation can be tuned by changing the surface chemistry of the support using different functional groups (butyl, carboxyl, or amino groups). The second approach includes using additional promoters (Cu, Fe, etc.), which we used to modify catalysts for conversion of different biomass-based derivatives [31,42,43].

3. Materials and Methods

3.1. Catalyst Preparation

The high-loading carbide catalyst Ni_{0.1}MoC-SiO₂ with an Ni/Mo molar ratio of 0.1 was prepared by the modified gel combustion method [15]. Ammonium molybdate tetrahydrate ((NH₄)₆Mo₇O₂₄·4H₂O, >98%, Reachim, Moscow, Russia) and nickel (II) nitrate hexahydrate (Ni(NO₃)₂·6H₂O, >98%, Reachim, Moscow, Russia) were used as Mo and Ni sources, while citric acid (C₆H₈O₇, >98%, Reachim, Moscow, Russia) was used as a complexation agent and as a source of carbon for the carbide formation. For the synthesis of the high-loading sample, the corresponding quantities of Ni and Mo salts in a mixture with citric acid were dissolved in water under vigorous stirring at 80 °C. Citric acid was taken in an amount equal to the molar sum of metals. When the homogeneous solution was obtained, ethyl silicate-32 ((C₂H₅O)₄Si, >98%, Reachim, Moscow, Russia) was added in an amount of 10 wt.% counted for the calcined sample. The solution was heated to form a viscous substance and dried at 100 °C. The ground powder of the obtained precursor was heated in a quartz reactor in the Ar flow at 400 °C for 2 h. The obtained sample was reduced at 600 °C in a hydrogen flow for 2 h. Each temperature treatment was accompanied by the passivation of the sample by ethanol at room temperature without air access.

The preparation of supported carbide catalysts was carried out in accordance with the incipient wetness impregnation technique and modified gel combustion method described above. (NH₄)₆Mo₇O₂₄·4H₂O, Ni(NO₃)₂·6H₂O, and citric acid were used to prepare the impregnating solution. Silica dioxide (SiO₂, >98%, Reachim, Moscow, Russia), aluminum oxide (Al₂O₃, Sasol, Sandton, South Africa), and the porous carbon material (C-Sibunit (BIC, Omsk, Russia)) were taken as supports in the synthesis of supported catalysts Ni_{0.1}MoC/X, where 0.1 was the molar ratio of Ni/Mo, and X was the support. To prepare the impregnating solution, a mixture of Ni and Mo salts with Ni/Mo molar ratio of 0.1 was dissolved with citric acid in water at 80 °C. The cooled solution was poured into a volumetric flask and diluted with water so that the summary metal concentration was 1.25 M. The synthesis of supported catalysts was carried out using incipient wetness impregnation. Before the procedure, all supports were dried at 200 °C. After impregnation, the total composition of the metals in the catalysts was 13 wt.%. The impregnated supports were dried at 80 °C in air, calcined in an argon atmosphere at 400 °C (2 h), cooled down, and passivated. The pretreated samples were reduced under hydrogen flow at 600 °C (2 h). Passivation with ethanol was performed at the end of each temperature treatment to avoid the catalyst oxidizing in air.

3.2. Catalytic Activity Tests

The study of the activity and selectivity of the catalysts in the process of furfural hydrogenation was carried out in a 300 mL stainless steel batch reactor (Parker Auto-

clave Engineers, Erie, PA, USA). Before the reaction, 1 g of catalyst (fine powder with size < 0.071 mm) was placed in an autoclave and activated in situ in 300 mL/min flow of H₂ at 350 °C for 60 min. Then, 60 mL of 3.5 vol.% furfural (C₅H₄O₂, >98%, ReaChem, Moscow, Russia) or furfuryl alcohol (>98%, Sigma-Aldrich, Burlington, USA) in isopropanol (C₃H₈O, >99%, ReaChem, Moscow, Russia) was added into the reactor at room temperature, and heated to 150 °C under a hydrogen atmosphere at 0.1 MPa. When the required temperature was reached, H₂ was fed into the reactor to reach 6.0 MPa. The stirring rate was 1800 rpm. During the whole process, samples were taken for analysis, and the pressure in the reactor was kept at 6.0 MPa.

The conversion of furfural without solvent over carbide catalyst was conducted in a fixed-bed flow reactor with a diameter of 1 cm, operating at 5.0 MPa H₂ pressure, and reaction temperatures of 160, 200, and 260 °C. The catalyst fraction (3 mL, mesh size of 0.25–0.5 mm) was diluted with 3 mL of quartz (mesh size of 0.25–0.5 mm) to avoid localized overheating. The sample was activated via in situ reduction in hydrogen flow (300 mL/min) at 350 °C for 1 h. After the activation stage, the reactor was cooled to the target temperature (160, 200, and 260 °C), and hydrogen was fed into the reactor (300 mL/min) to reach 5.0 MPa. Pure furfural/furfuryl alcohol was pumped into the reaction zone by HPLC (Kvarta LLC, Novosibirsk, Russia), with a flow rate of 3 mL/h. During the process, the resulting reaction mixture was accumulated in the collector for one hour, and then it was taken for analysis.

After each experiment, the catalyst was removed from the reactor and separated from the liquid phase by filtration. The samples were washed with acetone and dried at room temperature.

3.3. Products Analysis

The gas chromatography–mass spectrometer Agilent 7000B (Santa Clara, CA, USA) was used for qualitative analysis of reaction products; the Agilent 7000B was equipped with a triple quadrupole analyzer and quartz capillary column (CD Wax).

An Agilent Technologies GC-7820A gas chromatograph (Santa Clara, CA, USA) was used for quantitative analyses. The GC was equipped with a flame ionization detector (FID) and capillary column (HP-5 with stationary phase (5%-phenyl)-methyl polysiloxane, 30 m | 0.32 mm | 0.25 μm).

The furfural (F)/furfuryl alcohol (FA) conversion was determined as follows:

$$\text{Conversion} = \frac{C_{0,F/FA} - C_{t,F/FA}}{C_{0,F/FA}} \cdot 100\%$$

where $C_{0,F/FA}$ and $C_{t,F/FA}$ are the initial and current (at time t) furfural/furfuryl alcohol concentrations, respectively.

The yield of i product was calculated as follows:

$$\text{Yield}_i = \frac{C_{t,i}}{C_{0,F/FA}} \cdot 100\%$$

where $C_{t,i}$ is the concentration of i product at time t ; $C_{0,F/FA}$ is the initial concentration of furfural/furfuryl alcohol.

The selectivity of the formation of i product was calculated as the ratio of the current concentration of i product to the concentration of unreacted furfural/furfuryl alcohol:

$$\text{Selectivity}_i = \frac{C_{t,i}}{(C_{0,F/FA} - C_{t,F/FA})} \cdot 100\%$$

3.4. X-ray Diffraction

X-ray diffraction analysis on a Bruker D8 Advance X-ray diffractometer (Bruker Corporation, Berlin, Germany) was used for the study of the phase composition of Ni_{0.1}MoC-

based catalysts. The X-ray diffractometer was equipped with a Lynxeye linear detector. Monochromatic CuK α radiation ($\lambda = 1.5418 \text{ \AA}$) was applied for the analysis. XRD patterns were obtained in the 2θ range from 15° to 80° , with a step of 0.05° and accumulation time of 3 s at each point.

3.5. X-ray Photoelectron Spectroscopy

An XPS study was carried out using a photoelectron spectrometer (SPECS Surface Nano Analysis GmbH, Berlin, Germany). The spectrometer was equipped with a high-pressure cell that makes it possible to treat samples under gaseous mixtures. The spectra were measured using monochromatic Al K α radiation ($h\nu = 1486.74 \text{ eV}$). The relative concentrations of elements were determined from the integral intensities of the core-level spectra, using the cross sections according to Scofield [44]. The spectra were fitted into several components after background subtraction by the Shirley method [45]. Before the analysis, all of the catalysts were additionally reduced under 1.0 MPa of H $_2$ at 350°C for 30 min in the high-pressure cell.

3.6. X-ray Absorption Spectroscopy

The phase composition and structure of catalysts were investigated using X-ray absorption spectroscopy. The XAS study was carried out at the Structural Materials Science Station of the Kurchatov synchrotron radiation source (Kurchatov Institute, Moscow, Russia) [46] and the EXAFS spectroscopy beamline of the Siberian Synchrotron and Terahertz Radiation Center (Budker Institute of Nuclear Physics, Novosibirsk, Russia). The Mo K-edge and Ni K-edge spectra were processed using the DEMETER software package [47].

3.7. Elemental Analysis

The carbon content in the catalysts, before and after the reaction, was measured with a Vario El III elemental analyzer, CHNS version (Elementar Analysensysteme GmbH, Langenselbold, Germany).

3.8. Transmission Electron Microscopy

High-resolution transmission electron microscopy (HRTEM) was used to examine the structure and microstructure of the catalysts. For the measurements, a JEM-2010 electron microscope (JEOL, Tokyo, Japan) was used.

3.9. Texture Characteristics

The specific surface area (A_{BET}) of fresh catalysts and supports was calculated with the Brunauer–Emmett–Teller (BET) method, using nitrogen adsorption isotherms measured at liquid nitrogen. The nitrogen adsorption isotherms were measured with an automated volumetric adsorption ASAP 2400 sorptometer (Micromeritics Instrument Corp., Norcross, GA, USA). Prior to taking the measurements, the samples were outgassed at 150°C at a pressure 0.13 Pa for 4 h.

4. Conclusions

This study indicated that a high-loading catalyst Ni $_{0.1}$ MoC-SiO $_2$ containing a cubic molybdenum carbide modified with nickel metal particles provided a 31 mol.% yield of 2-methylfuran in furfural hydrogenation at 150°C under a hydrogen pressure of 6.0 MPa in a batch reactor. An Ni/Mo ratio of 0.1 was used to synthesize the supported catalyst using a combination of gel combustion and insipient wetness impregnation methods. The study of catalysts with 13 wt.% of active phase Ni $_{0.1}$ MoC supported on SiO $_2$, Al $_2$ O $_3$ and porous carbon material (C) showed higher activity in furfural conversion compared with the high-loading catalyst. The carbide materials supported on C showed a 100 mol.% conversion of furfural, with a yield of 61 mol.% of 2-MF after 3.5 h in a batch reactor at 150°C under 6.0 MPa hydrogen pressure. Using different physical–chemical methods (XRD, XPS, XANES, and EXAFS analyses), it was confirmed that during the thermal treatment

of the Ni_{0.1}MoC/X precursors, the formation of carbides (hcp-Mo₂C and fcc-MoC_{1-x}) and metallic nickel as active components occurred. Molybdenum oxide was also detected; however, the formation of this oxide may have been related to the oxidation of the catalysts by oxygen present in the air after the reduction stage. The Ni_{0.1}MoC/C catalyst was tested for furfural hydrogenation in a batch reactor at 150 °C under a hydrogen pressure of 6.0 MPa with the formation of 2-methylfuran (yield of 58 mol.%).

It was established that hydrogenation of solvent-free furfuryl alcohol over Ni_{0.1}MoC/C catalyst in a fixed-bed reactor led to the formation of 2-methylfuran with a yield of 82 mol.% in a temperature range of 160–200 °C and a hydrogen pressure of 5.0 MPa. At the same time, the temperature of 260 °C was too high for producing 2-methylfuran, and led to the formation of 2-MTHF, pentanols, and n-pentane. In contrast, the hydrogenation of solvent-free furfural at 260 °C resulted in 100 mol.% conversion, and a yield of 2-MF of up to 86 mol.%.

Author Contributions: Conceptualization, A.S. and V.A.Y.; methodology, A.S. and M.V.A.; formal analysis, I.N.S.; investigation, I.N.S., O.A.B. and A.A.S.; writing—original draft preparation, A.S.; writing—review and editing, V.A.Y.; visualization, M.V.A. All authors have read and agreed to the published version of the manuscript.

Funding: This work was supported by the Ministry of Science and Higher Education of the Russian Federation (Agreement No. 075-15-2022-263).

Data Availability Statement: Not applicable.

Acknowledgments: The TEM study was carried out using facilities of the shared research center “National center of investigation of catalysts” at the Boreskov Institute of Catalysis. The investigations were performed using large-scale research facilities “EXAFS spectroscopy beamline” at the Siberian Synchrotron and Terahertz Radiation Center.

Conflicts of Interest: The authors declare no conflict of interest.

References

1. Yeletsky, P.M.; Kukushkin, R.G.; Alekseeva, M.V.; Smirnov, A.A. CHAPTER 6: Application of Heterogeneous Catalysts for the Conversion of Biomass-Derived Feedstocks into Fuel Components and Eco-Additives. *Heterog. Catal. Energy Appl.* **2020**, *6*, 150–179. [[CrossRef](#)]
2. Hoydonckx, H.E.; Van Rhijn, W.M.; Van Rhijn, W.; De Vos, D.E.; Jacobs, P.A. Furfural and Derivatives. In *Ullmann's Encyclopedia of Industrial Chemistry*; Wiley-VCH Verlag GmbH & Co. KGaA.: Hoboken, NJ, USA, 2007; eISBN 9783527306732. [[CrossRef](#)]
3. Thewes, M.; Muether, M.; Pischinger, S.; Budde, M.; Brunn, A.; Sehr, A.; Adomeit, P.; Klankermayer, J. Analysis of the Impact of 2-Methylfuran on Mixture Formation and Combustion in a Direct-Injection Spark-Ignition Engine. *Energy Fuels* **2011**, *25*, 5549–5561. [[CrossRef](#)]
4. Lange, J.-P.; van der Heide, E.; van Buijtenen, J.; Price, R. Furfural-A Promising Platform for Lignocellulosic Biofuels. *Chemsuschem* **2012**, *5*, 150–166. [[CrossRef](#)] [[PubMed](#)]
5. Dutta, S.; De, S.; Saha, B.; Alam, I. Advances in Conversion of Hemicellulosic Biomass to Furfural and Upgrading to Biofuels. *Catal. Sci. Technol.* **2012**, *2*, 2025–2036. [[CrossRef](#)]
6. Gürbüz, E.I.; Gallo, J.M.R.; Alonso, D.M.; Wettstein, S.G.; Lim, W.Y.; Dumesic, J.A. Conversion of Hemicellulose into Furfural Using Solid Acid Catalysts in γ -Valerolactone. *Angew. Chem. Int. Ed.* **2013**, *52*, 1270–1274. [[CrossRef](#)]
7. Hoang, A.T.; Pham, V.V. 2-Methylfuran (MF) as a potential biofuel: A thorough review on the production pathway from biomass, combustion progress, and application in engines. *Renew. Sustain. Energy Rev.* **2021**, *148*, 111265. [[CrossRef](#)]
8. Wang, Y.; Zhao, D.; Rodríguez-Padrón, D.; Len, C. Recent Advances in Catalytic Hydrogenation of Furfural. *Catalysts* **2019**, *9*, 796. [[CrossRef](#)]
9. Burnett, L.W.; Johns, I.B.; Holdren, R.F.; Hixon, R.M. Production of 2-Methylfuran by Vapor-Phase Hydrogenation of Furfural. *Ind. Eng. Chem.* **1948**, *40*, 502–505. [[CrossRef](#)]
10. Nguyen-Huy, C.; Kim, J.S.; Yoon, S.; Yang, E.; Kwak, J.H.; Lee, M.S.; An, K. Supported Pd nanoparticle catalysts with high activities and selectivities in liquid-phase furfural hydrogenation. *Fuel* **2018**, *226*, 607–617. [[CrossRef](#)]
11. Mäkelä, E.; Lahti, R.; Jaatinen, S.; Romar, H.; Hu, T.; Puurunen, R.L.; Lassi, U.; Karinen, R. Study of Ni, Pt, and Ru Catalysts on Wood-based Activated Carbon Supports and their Activity in Furfural Conversion to 2-Methylfuran. *ChemCatChem* **2018**, *10*, 3269–3283. [[CrossRef](#)]
12. Jaatinen, S.K.; Karinen, R.; Lehtonen, J.S. Liquid Phase Furfural Hydrotreatment to 2-Methylfuran with Carbon Supported Copper, Nickel, and Iron Catalysts. *ChemistrySelect* **2017**, *2*, 51–60. [[CrossRef](#)]

13. Hutchings, G.S.; Luc, W.; Lu, Q.; Zhou, Y.; Vlachos, D.G.; Jiao, F. Nanoporous Cu–Al–Co Alloys for Selective Furfural Hydrodeoxygenation to 2-Methylfuran. *Ind. Eng. Chem. Res.* **2017**, *56*, 3866–3872. [[CrossRef](#)]
14. Smirnov, A.; Geng, Z.; Khromova, S.; Zavarukhin, S.; Bulavchenko, O.; Saraev, A.; Kaichev, V.; Ermakov, D.; Yakovlev, V. Nickel molybdenum carbides: Synthesis, characterization, and catalytic activity in hydrodeoxygenation of anisole and ethyl caprate. *J. Catal.* **2017**, *354*, 61–77. [[CrossRef](#)]
15. Shilov, I.N.; Smirnov, A.A.; Bulavchenko, O.A.; Yakovlev, V.A. Effect of Ni–Mo Carbide Catalyst Formation on Furfural Hydrogenation. *Catalysts* **2018**, *8*, 560. [[CrossRef](#)]
16. Burueva, D.B.; Smirnov, A.A.; Bulavchenko, O.A.; Prosvirin, I.P.; Gerasimov, E.Y.; Yakovlev, V.A.; Kovtunov, K.V.; Koptuyg, I.V. Pairwise Parahydrogen Addition Over Molybdenum Carbide Catalysts. *Top. Catal.* **2020**, *63*, 2–11. [[CrossRef](#)]
17. Lee, W.-S.; Wang, Z.; Zheng, W.; Vlachos, D.; Bhan, A. Vapor phase hydrodeoxygenation of furfural to 2-methylfuran on molybdenum carbide catalysts. *Catal. Sci. Technol.* **2014**, *4*, 2340–2352. [[CrossRef](#)]
18. Xiong, K.; Lee, W.-S.; Bhan, A.; Chen, J.G. Molybdenum Carbide as a Highly Selective Deoxygenation Catalyst for Converting Furfural to 2-Methylfuran. *ChemSusChem* **2014**, *7*, 2146–2149. [[CrossRef](#)]
19. McManus, J.R.; Vohs, J.M. Deoxygenation of glycolaldehyde and furfural on Mo₂C/Mo(100). *Surf. Sci.* **2014**, *630*, 16–21. [[CrossRef](#)]
20. Hu, Z.; Zhang, L.; Huang, J.; Feng, Z.; Xiong, Q.; Ye, Z.; Chen, Z.; Li, X.; Yu, Z. Self-supported nickel-doped molybdenum carbide nanoflower clusters on carbon fiber paper for an efficient hydrogen evolution reaction. *Nanoscale* **2021**, *13*, 8264–8274. [[CrossRef](#)]
21. Wang, X.; Zhang, J.; Wang, Z.; Lin, Z.; Shen, S.; Zhong, W. Fabricating Ru single atoms and clusters on CoP for boosted hydrogen evolution reaction. *Chin. J. Struct. Chem.* **2023**, 100035. [[CrossRef](#)]
22. Wang, Z.; Lin, Z.; Wang, Y.; Shen, S.; Zhang, Q.; Wang, J.; Zhong, W. Nontrivial Topological Surface States in Ru₃Sn₇ toward Wide pH-Range Hydrogen Evolution Reaction. *Adv. Mater.* **2023**, 2302007. [[CrossRef](#)]
23. Smirnov, A.A.; Selishcheva, S.A.; Yakovlev, V.A. Acetalization Catalysts for Synthesis of Valuable Oxygenated Fuel Additives from Glycerol. *Catalysts* **2018**, *8*, 595. [[CrossRef](#)]
24. Magar, S.; Kamble, S.; Mohanraj, G.T.; Jana, S.K.; Rode, C. Solid-Acid-Catalyzed Etherification of Glycerol to Potential Fuel Additives. *Energy Fuels* **2017**, *31*, 12272–12277. [[CrossRef](#)]
25. Aguado-Deblas, L.; Estevez, R.; Russo, M.; La Parola, V.; Bautista, F.M.; Testa, M.L. Microwave-Assisted Glycerol Etherification Over Sulfonic Acid Catalysts. *Materials* **2020**, *13*, 1584. [[CrossRef](#)]
26. Liu, Y.; Ma, X.; Wang, S.; Gong, J. The nature of surface acidity and reactivity of MoO₃/SiO₂ and MoO₃/TiO₂-SiO₂ for transesterification of dimethyl oxalate with phenol: A comparative investigation. *Appl. Catal. B Environ.* **2007**, *77*, 125–134. [[CrossRef](#)]
27. Rajagopal, S.; Marzari, J.; Miranda, R. Silica-Alumina-Supported Mo Oxide Catalysts: Genesis and Demise of Brønsted-Lewis Acidity. *J. Catal.* **1995**, *151*, 192–203. [[CrossRef](#)]
28. Ma, X.; Gong, J.; Wang, S.; Gao, N.; Wang, D.; Yang, X.; He, F. Reactivity and surface properties of silica supported molybdenum oxide catalysts for the transesterification of dimethyl oxalate with phenol. *Catal. Commun.* **2004**, *5*, 101–106. [[CrossRef](#)]
29. Fuente-Hernández, A.; Lee, R.; Béland, N.; Zamboni, I.; Lavoie, J.-M. Reduction of Furfural to Furfuryl Alcohol in Liquid Phase over a Biochar-Supported Platinum Catalyst. *Energies* **2017**, *10*, 286. [[CrossRef](#)]
30. Li, C.P.; Proctor, A.; Hercules, D.M. Curve Fitting Analysis of ESCA Ni2p Spectra of Nickel-Oxygen Compounds and Ni/Al₂O₃Catalysts. *Appl. Spectrosc.* **1984**, *38*, 880–886. [[CrossRef](#)]
31. Khromova, S.A.; Smirnov, A.A.; Bulavchenko, O.A.; Saraev, A.A.; Kaichev, V.V.; Reshetnikov, S.I.; Yakovlev, V.A. Anisole hydrodeoxygenation over Ni–Cu bimetallic catalysts: The effect of Ni/Cu ratio on selectivity. *Appl. Catal. A Gen.* **2014**, *470*, 261–270. [[CrossRef](#)]
32. Smirnov, A.; Khromova, S.; Ermakov, D.; Bulavchenko, O.; Saraev, A.; Aleksandrov, P.; Kaichev, V.; Yakovlev, V. The composition of Ni–Mo phases obtained by NiMoO_x-SiO₂ reduction and their catalytic properties in anisole hydrogenation. *Appl. Catal. A Gen.* **2016**, *514*, 224–234. [[CrossRef](#)]
33. Bearden, J.A.; Burr, A.F. Reevaluation of X-ray Atomic Energy Levels. *Rev. Mod. Phys.* **1967**, *39*, 125–142. [[CrossRef](#)]
34. Chen, W.-F.; Wang, C.-H.; Sasaki, K.; Marinkovic, N.; Xu, W.; Muckerman, J.T.; Zhu, Y.; Adzic, R.R. Highly active and durable nanostructured molybdenum carbide electrocatalysts for hydrogen production. *Energy Environ. Sci.* **2013**, *6*, 943–951. [[CrossRef](#)]
35. He, C.; Tao, J. Exploration of the electrochemical mechanism of ultrasmall multiple phases molybdenum carbides nanocrystals for hydrogen evolution reaction. *RSC Adv.* **2016**, *6*, 9240–9246. [[CrossRef](#)]
36. Rochet, A.; Baubet, B.; Moizan, V.; Devers, E.; Hugon, A.; Pichon, C.; Payen, E.; Briois, V. Influence of the Preparation Conditions of Oxidic NiMo/Al₂O₃ Catalysts on the Sulfidation Ability: A Quick-XAS and Raman Spectroscopic Study. *J. Phys. Chem. C* **2015**, *119*, 23928–23942. [[CrossRef](#)]
37. Ressler, T. Bulk Structural Investigation of the Reduction of MoO₃ with Propene and the Oxidation of MoO₂ with Oxygen. *J. Catal.* **2002**, *210*, 67–83. [[CrossRef](#)]
38. Preda, I.; Soriano, L.; Díaz-Fernández, D.; Domínguez-Cañizares, G.; Gutiérrez, A.; Castro, G.R.; Chaboy, J. X-ray absorption study of the local structure at the NiO/oxide interfaces. *J. Synchrotron Radiat.* **2013**, *20*, 635–640. [[CrossRef](#)]
39. Kang, J.-X.; Zhang, D.-F.; Guo, G.-C.; Yu, H.-J.; Wang, L.; Huang, W.-F.; Wang, R.-Z.; Guo, L.; Han, X.-D. Au Catalyzed Carbon Diffusion in Ni: A Case of Lattice Compatibility Stabilized Metastable Intermediates. *Adv. Funct. Mater.* **2018**, *28*, 1706434. [[CrossRef](#)]

40. Guerrero-Torres, A.; Jiménez-Gómez, C.P.; Cecilia, J.A.; García-Sancho, C.; Quirante-Sánchez, J.J.; Mérida-Robles, J.M.; Maireles-Torres, P. Influence of the Incorporation of Basic or Amphoteric Oxides on the Performance of Cu-Based Catalysts Supported on Sepiolite in Furfural Hydrogenation. *Catalysts* **2019**, *9*, 315. [[CrossRef](#)]
41. German, D.; Kolobova, E.; Pakrieva, E.; Carabineiro, S.A.C.; Sviridova, E.; Perevezentsev, S.; Alijani, S.; Villa, A.; Prati, L.; Postnikov, P.; et al. The Effect of Sibunit Carbon Surface Modification with Diazonium Tosylate Salts of Pd and Pd-Au Catalysts on Furfural Hydrogenation. *Materials* **2022**, *15*, 4695. [[CrossRef](#)]
42. Smirnov, A.A.; Shilov, I.N.; Bulavchenko, O.A.; Saraev, A.; Yakovlev, V.A. Hydrotreatment of Anisole and Furfural as Model Compounds of Bio-oil over Chromium Modified Nickel-Based Catalysts. *ChemistrySelect* **2019**, *4*, 7317–7326. [[CrossRef](#)]
43. Selishcheva, S.A.; Smirnov, A.A.; Fedorov, A.V.; Bulavchenko, O.A.; Saraev, A.A.; Lebedev, M.Y.; Yakovlev, V.A. Highly Active CuFeAl-containing Catalysts for Selective Hydrogenation of Furfural to Furfuryl Alcohol. *Catalysts* **2019**, *9*, 816. [[CrossRef](#)]
44. Scofield, J.H. Hartree-Slater Subshell Photoionization Cross-Sections at 1254 and 1487 eV. *Electron Spectrosc. Relat. Phenom.* **1976**, *8*, 129–137. [[CrossRef](#)]
45. Shirley, D.A. High-Resolution X-Ray Photoemission Spectrum of the Valence Bands of Gold. *Phys. Rev. B* **1972**, *5*, 4709–6024. [[CrossRef](#)]
46. Chernyshov, A.; Veligzhanin, A.; Zubavichus, Y. Structural Materials Science end-station at the Kurchatov Synchrotron Radiation Source: Recent instrumentation upgrades and experimental results. *Nucl. Instrum. Methods Phys. Res. Sect. A Accel. Spectrometers Detect. Assoc. Equip.* **2009**, *603*, 95–98. [[CrossRef](#)]
47. Ravel, B.; Newville, M. ATHENA, ARTEMIS, HEPHAESTUS: Data Analysis for X-ray Absorption Spectroscopy Using IFFEF-FIT. *J. Synchrotron Radiat.* **2005**, *12*, 537–541. [[CrossRef](#)]

Disclaimer/Publisher's Note: The statements, opinions and data contained in all publications are solely those of the individual author(s) and contributor(s) and not of MDPI and/or the editor(s). MDPI and/or the editor(s) disclaim responsibility for any injury to people or property resulting from any ideas, methods, instructions or products referred to in the content.